Urban Climate 65 (2026) 102742

Contents lists available at ScienceDirect

Urban Climate

journal homepage: www.elsevier.com/locate/uclim

Heat vulnerability in the City of Ponce, Puerto Rico

Laura T. Cabrera-Rivera [a], Frank E. Muller-Karger [b], Digna Rueda-Roa [b], Heriberto Marin [c], Tischa A. Muñoz-Erickson [d], Pablo A. Méndez-Lázaro [a,e,*]

[a] Environmental Health Department, Graduate School of Public Health, University of Puerto Rico-Medical Sciences Campus, United States of America
[b] Institute for Marine Remote Sensing/ImaRS, College of Marine Science, University of South Florida, United States of America
[c] Department of Health Services Administration, Graduate School of Public Health, University of Puerto Rico – Medical Sciences Campus, United States of America
[d] USDA Forest Service, International Institute of Tropical Forestry, United States of America
[e] University of Puerto Rico-Cancer Biology, Division and Environmental Translational Cancer Program- Comprehensive Cancer Center, United States of America

ARTICLE INFO

Keywords:
Urban heat island
Land surface temperature
Caribbean
Puerto Rico
Public health
Green infrastructure

ABSTRACT

This study assessed heat vulnerability in the city of Ponce, Puerto Rico, by integrating satellite-derived land surface temperature (LST) data with demographic and socioeconomic indicators. Spatial analysis, principal component analysis (PCA), and multivariate regression were applied to develop a Heat Vulnerability Index (HVI) that maps heat risk across urban neighborhoods. Environmental variables, LST, Normalized Difference Vegetation Index (NDVI), impervious surface cover, slope, and elevation, were analyzed alongside indicators such as age, disability, living alone, poverty, and unemployment to identify key drivers of heat exposure, social isolation, and vulnerability. Multivariate regression analysis showed that lower vegetation, greater impervious surface, lower elevation, and a small cooling effect from slope were significantly associated with higher LST, explaining over 80 % of temperature variability. Results show that census tracts classified as High Vulnerability consistently experienced elevated temperatures and were characterized by higher concentrations of elderly individuals, people with disabilities, and socially isolated residents. These high vulnerability census tracts, where extreme heat and social disadvantage converge, represent areas where immediate heat mitigation actions may be most effective. Green infrastructure investments (e.g., urban greening), targeted adaptation strategies (e.g., cooling centers, community outreach), and urban planning policies are likely to reduce risk and improve resilience in high vulnerability areas. This research provides actionable insights for city planners, public health officials, and policymakers to protect the lives, health, and well-being of residents in Ponce amid a changing environment.

1. Introduction

Extreme weather events, particularly extreme heat events, present unprecedented challenges for public health in cities and other communities (Ipcc, 2022; Méndez-Lázaro, 2023), with 2023 and 2024 recorded as the two hottest years on record (Copernicus, 2025;

* Corresponding author at: Department of Environmental Health, University of Puerto Rico, Medical Sciences Campus, San Juan, PR 00921, United States of America.

E-mail addresses: Laura.cabrera@upr.edu (L.T. Cabrera-Rivera), carib@usf.edu (F.E. Muller-Karger), heriberto.marin@upr.edu (H. Marin), tischa.a.munoz-erickson@usda.gov (T.A. Muñoz-Erickson), pablo.mendez1@upr.edu (P.A. Méndez-Lázaro).

https://doi.org/10.1016/j.uclim.2025.102742
Received 21 June 2025; Received in revised form 19 November 2025; Accepted 8 December 2025
Available online 17 January 2026
2212-0955/

NASA, 2025; NOAA, 2025; WMO, 2025). These temperature extremes are exacerbated in urban areas by the urban heat island (UHI) effect, where buildings, roads, and other heat-absorbing surfaces retain heat and reduce natural cooling, making cities notably warmer than surrounding rural regions (Kim and Brown, 2021; Rizwan et al., 2008; Devanathan and Devanathan, 2011; Mohajerani et al., 2017). The UHI effect increasingly threatens infrastructure resilience (Meenar et al., 2023; Aboulnaga et al., 2024), creating challenges for managing heat-related stress on infrastructure while safeguarding populations, particularly in regions with limited resources and aging infrastructure (Niggli et al., 2022; Zhou et al., 2020). These environmental and social challenges call for innovative approaches to protect public health and promote resilient, environmentally responsible, and socially equitable cities.

Puerto Rico exemplifies these challenges, particularly in its small cities, such as Ponce (Méndez-Lázaro, 2023). To date, most heat-related research on the island of Puerto Rico has focused on the capital city of San Juan (Méndez-Lázaro et al., 2018a), leaving knowledge gaps about other vulnerable municipalities. As the largest and most populated municipality in Puerto Rico in the southern region (Bureau UC, 2025), Ponce confronts unique challenges. This city is characterized by higher temperatures than other locations in Puerto Rico (Puleikis and Wang, 2023) and presents an important case where environmental heat stress coincides with significant socioeconomic vulnerability.

Several socioeconomic and demographic indicators help to evaluate heat vulnerability in this area. Income and poverty levels directly affect the ability of residents to afford cooling technologies and recover from extreme heat events (Osberghaus and Abeling, 2022). The educational level can influence awareness of and access to heat adaptation resources, such as air conditioning, cooling centers, public health alerts, and programs that provide financial support for home modifications like weatherization or cooling system installation (He et al., 2022). Disability status and age demographics are populations that may face heightened physiological vulnerability to heat stress and may require additional support during extreme heat events (Ji et al., 2025). A comparative analysis of socioeconomic indicators across Puerto Rico's major urban areas and the US presents considerable disparities, as shown in Table 1. In general, the city of Ponce exhibits substantially lower average income and higher poverty levels than both the U.S. and the overall Puerto Rico population. It also has a larger proportion of residents with disabilities and senior citizens (Table 1). These groups are especially susceptible to heat-related health impacts.

Ponce and southern Puerto Rico experience higher temperatures compared to the northern region (Puleikis and Wang, 2023). While San Juan's average maximum land surface temperatures range from 39 °C to 55 °C, Ponce regularly experiences land surface temperatures ranging from 44 °C to 57 °C. These regional differences are attributed to topographical features, prevailing wind patterns, and local climatological conditions (Puleikis and Wang, 2023). The southern region's higher baseline temperatures and this accelerating warming trend make it particularly vulnerable to extreme heat events.

The infrastructure of the municipality of Ponce includes many aging buildings, limited green infrastructure, and inconsistent access to cooling resources, which mainly affects its vulnerable populations (Sánchez-Celada, 2018). These physical constraints coincide with elevated rates of heat-exacerbated health conditions, such as cardiovascular disease and cancer, compared to other municipalities in Puerto Rico (*Interactive Atlas of Heart Disease and Stroke*, 2025). The unreliable electricity supply further compounds these challenges, as power outages during heat events leave at-risk populations without access to cooling systems (Puerto Rico Climate Change Council (PRCCC), 2022; Redacción, 2024; *Fin de Semana Sin Luz para Sectores de San Juan y Ponce – Metro Puerto Rico*, 2025; *Sin Luz Gran Parte de Ponce - Primera Hora*, 2025; *Camión Deja Sin Luz a Comunidad de Ponce – Telemundo Puerto Rico*, 2025; *Alcaldesa de ponce advierte que LUMA está "matando a nuestra gente"*, 2025).

Satellite information and other scientific observations have emerged as tools to help assess urban heat maps, particularly in regions with limited ground monitoring capabilities. Previous studies have successfully employed satellite-derived land surface temperature data to map urban heat patterns and identify vulnerable areas (Méndez-Lázaro et al., 2018a; Bu et al., 2024). Hulley et al. (2020) demonstrated the effectiveness of thermal sensors in developing high-resolution heat vulnerability indices (HVIs) at sub-city block scales in Los Angeles, combining temperature data with socio-demographic information and vegetation metrics (Hulley et al., 2019). Méndez-Lázaro et al. (2018) developed HVI models for San Juan by integrating satellite-derived thermal data with social vulnerability indicators (Méndez-Lázaro et al., 2018a). These approaches are valuable in regions where traditional temperature monitoring networks may be sparse or inconsistent.

This study developed an urban heat vulnerability assessment by integrating satellite-derived earth observations and social determinants of health (Méndez-Lázaro et al., 2018a; Bu et al., 2024). The primary objective was to evaluate the interdependencies between such determinants and the areas of high and low heat in the city of Ponce and to develop a targeted HVI to help local community leaders develop adaptive options to enhance resilience against extreme heat events.

This paper outlines the methodology used for the heat vulnerability assessment. It illustrates the value of integrating social equity

Table 1
Socioeconomic and demographic profile of the US, Puerto Rico, San Juan and Ponce.

	US[a]	Puerto Rico[a]	San Juan[a]	Ponce[a]
Median Household Income	$80,610	$24,112	$26,111	$17,700
Poverty[b]	11.5 %	41.7 %	39.5 %	53.2 %
Bachelor's Degree or Higher	37.7 %	29.8 %	41.3 %	28.2 %
Disabled Population	13.4 %	24.6 %	24.5 %	26.4 %
65 Years and Older	16.8 %	23.5 %	25.6 %	25.4 %

[a] Data obtained from the most recent Census.
[b] The 150 % of poverty estimate per census tract represents households whose income is 1.5 times (or 150 % of) the federal poverty level.

considerations into urban heat adaptation planning and offers evidence-based strategies for developing resilient urban infrastructure systems that protect vulnerable populations from extreme heat.

2. Methodology

2.1. Study area

The city of Ponce is located in the southern-central coastal region of Puerto Rico (see Fig. 1) (*Ponce Latitude Longitude*, 2025). Ponce is often referred to as “La Perla del Sur” (“The Pearl of the South”). It is one of the largest cities in Puerto Rico, with a population of approximately 132,138 inhabitants as of 2022 (*U.S. Census Bureau QuickFacts: Ponce Municipio, Puerto Rico*, 2025). Since 2010, Ponce's population has decreased to around 22.05 %, from 166,327 (2010) to 129,659 (2025) (*U.S. Census Bureau QuickFacts: Ponce Municipio, Puerto Rico*, 2025). This decline reflects broader demographic trends across Puerto Rico, driven by prolonged economic recession, limited job opportunities, high poverty rates, and outmigration, especially among younger residents seeking better conditions in the mainland United States (Giraldo-Santiago et al., 2024; Reyes Cruz, 2023). Natural disasters, such as Hurricane María, have also accelerated this population loss.

The city of Ponce has 114.9 mile^2 of land area. The city is located between the Caribbean Sea to the south and the Cordillera Central (Central Mountain Range) to the north. The region has a tropical maritime climate, with an annual maximum normal temperature of about 33.2 °C (91.8 °F) (US Department of Commerce N. PR and USVI Normals, 2025). Over a 30-year period, from the baseline of 1950–1979 to the more recent period of 1989–2019, air temperatures in southern and eastern Puerto Rico increased by approximately 0.6–1.1 °C (1–2 °F), with the most pronounced warming observed in lowland coastal areas such as Ponce (Puleikis and Wang, 2023).

2.2. Data acquisition

The study integrates four open-source data streams to develop a comprehensive heat vulnerability assessment. First, socio-demographic data were obtained from the U.S. Census Bureau's American Community Survey (2018–2022). This provided tract-level census information on vulnerability indicators, including age distribution, poverty levels, unemployment, living alone, and disability status (Méndez-Lázaro et al., 2018a). Census tracts are small, relatively permanent statistical subdivisions of counties designed to be relatively homogeneous units with respect to population characteristics, economic status, and living conditions, with an optimal population of 4000 residents (Méndez-Lázaro et al., 2018a). Second, vegetation coverage and impervious surfaces were identified using high-resolution satellite imagery. Normalized Difference Vegetation Index (NDVI) was derived from Landsat 8 Operational Land Imager (OLI) using the red and near-infrared bands (NIR-Red)/(NIR + Red) and averaged annually from 2014 to 2023. This provided a standardized measure of vegetation density ranging from −1 to 1, with higher values indicating denser vegetation. Impervious surface data were obtained from NOAA's 2022 Coastal Change Analysis Program (C-CAP), which provides land cover classification at 30 m spatial resolution (Cook et al., 2014). Third, land surface temperature (LST) data were estimated using

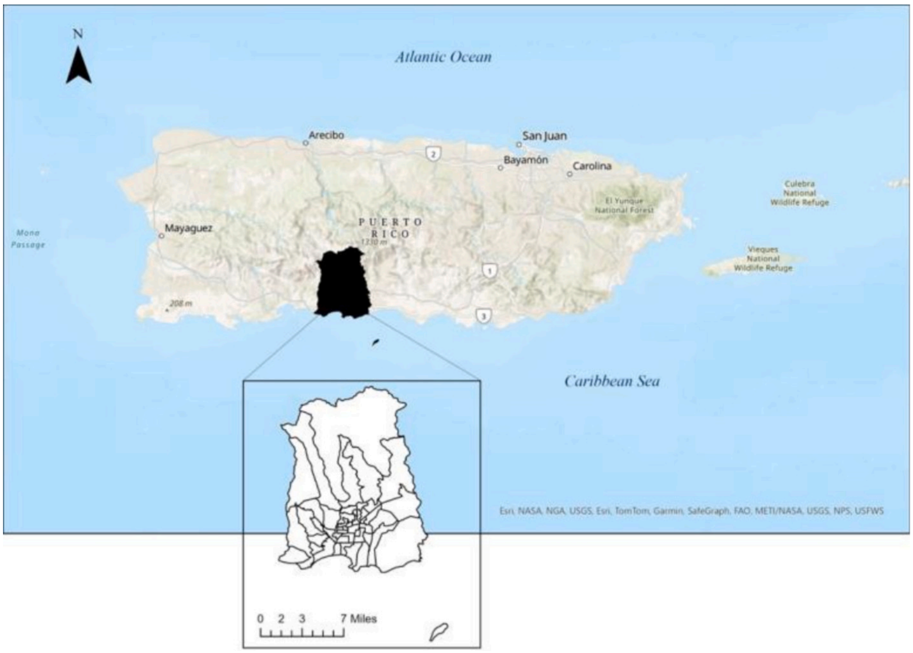

Fig. 1. Location and census tracts of Ponce, Puerto Rico.

Landsat 8's Thermal Infrared Sensor (TIRS) Band 10 (10.60–11.19 μm), providing thermal imagery at 100 m spatial resolution, resampled to 30 m. Surface temperature values were derived using a split-window algorithm incorporating atmospheric correction parameters and surface emissivity values (Méndez-Lázaro et al., 2018a). The analysis focused on imagery collected during the warmest months (June through September) from 2013 to 2023, capturing peak temperature patterns in the city of Ponce. All individual LST estimates collected each year were averaged across all years for the analyses presented here. Fourth, elevation data was incorporated using a high-resolution Digital Elevation Model (DEM) from 2022 of the U.S. Geological Survey (USGS), which provides elevation values at 10 m spatial resolution. This allowed for an assessment of topographic influences on land surface temperature.

Data quality was ensured through rigorous preprocessing protocols, including the exclusion of images with cloud coverage exceeding 25 % using Google Earth Engine's cloud-masking algorithms (Méndez-Lázaro et al., 2018a). The resulting LST dataset provides comprehensive coverage of temperature patterns across Ponce's urban landscape, enabling detailed analysis of urban heat distribution.

2.3. Statistical analysis

The analytical framework employed a two-stage statistical approach. First, Principal Component Analysis (PCA) was used to explore relationships among socio-demographic and environmental variables, identifying key factors contributing to heat vulnerability (Conlon et al., 2020). PCA enables dimension reduction while preserving essential patterns in the multivariate dataset, helping determine appropriate weights for the vulnerability index construction. Variables were standardized before PCA to account for different measurement scales.

Following the PCA, individual correlation analyses were conducted at the census tract level to assess any relationships between LST and key environmental variables, including NDVI, impervious surface coverage, and elevation. These analyses examined the bivariate relationships between these variables at the administrative unit scale to understand broad patterns of association.

For a more detailed spatial analysis, we modeled the environmental and geophysical of LST at the Landsat pixel level (30 m resolution). All predictor rasters (impervious surface, NDVI, and DEM) were resampled to the LST grid (30 m). From the DEM, we derived slope (in degrees) as a topographic metric to represent geological influences on surface heating. All predictors were standardized (z-scores) before modeling to enable comparison of coefficients, while LST was retained on its original temperature scale (°C).

This pixel-level multivariate regression model can be expressed as:

$$\text{LST} = \beta_0 + \beta_1(\text{Impervious}) + \beta_2(\text{DEM}) + \beta_3\ (\text{NDVI}) + \beta_4\ (\text{Slope}) + \varepsilon$$

Where:

- LST represents the average land surface temperature (°C) derived from Landsat 8 TIRS Band 10.
- Impervious represents the mean percentage (0–1) of impervious surface coverage derived from NOAA's C-CAP program
- DEM represents the mean elevation (meters above sea level) obtained from USGS digital elevation model (DEM) data
- NDVI represents the normalized difference vegetation index derived from Landsat 8 OLI bands
- Slope represents the steepness of terrain (degrees), derived from the DEM.
- β_0-β_4 are the regression coefficients
- ε represents the error term

To visualize the topographic gradient of surface heating, a north–south transect was extracted across the study area. Elevation and mean land surface temperature (LST) values were sampled along this transect, and a smoothed moving-average curve was applied to highlight the general relationship between elevation and surface temperature. The analysis was conducted using R (version 4.1.1), and standard diagnostic tests were applied to verify model assumptions, including the normality of residuals, homoscedasticity, and the absence of multicollinearity.

For analytical purposes, census tracts were classified into three vulnerability categories (low, moderate, and high) based on terciles of the final Heat Vulnerability Index (HVI), a composite measure integrating land surface temperature, population density, and socio-demographic factors related to heat sensitivity (see HVI computation method in the next section). This classification divided the study area into three approximately equal groups representing different levels of heat-related risk. Statistical tests were conducted on key social and environmental variables to determine whether significant differences existed between high- and low-vulnerability areas. These statistical comparisons between high and low vulnerability areas serve a crucial practical purpose in identifying which social and environmental factors most strongly differentiate areas of concern. The Shapiro-Wilk test was used to assess the normality of distribution for each variable within the vulnerability groups. For variables with normal distributions ($p > 0.05$), independent samples *t*-tests were performed to compare means between high and low vulnerability areas. For non-normally distributed variables, non-parametric Wilcoxon rank-sum tests were used. Statistical significance was established at $p < 0.05$. The variables analyzed included population density, poverty rates, unemployment, age distribution (percentage over 65), disability status, percentage of single-person households, and land surface temperature.

These statistical methods provided a quantitative foundation for understanding the relationships between urban landscape characteristics and heat vulnerability patterns, which inform the subsequent development of the heat vulnerability index (Niu et al., 2021).

2.4. Heat vulnerability index

The HVI was developed following the methodological approach established by Méndez-Lázaro et al. (2017 and Bu et al. (2024) (Méndez-Lázaro et al., 2018a; Bu et al., 2024). We integrated two domains at the census tract level: sensitivity, referring to population characteristics that affect susceptibility to heat-related health impacts (poverty, unemployment, age $\geq$ 65, disability, and living alone), and exposure, referring to environmental conditions that indicate potential contact with extreme heat (mean land surface temperature and population density). Following vulnerability theory, we adopted a balanced scheme in which 50 % weight was assigned to exposure and 50 % to sensitivity. All variables were standardized, and directionality was harmonized so that higher values indicate greater vulnerability (Table 2).

To evaluate robustness, we also constructed two alternative indices. First, an equal-weights index in which all variables contributed equally, consistent with the San Juan HVI method (Méndez-Lázaro et al., 2018a). Second, a PCA-weighted index, in which principal component loadings were used as weights. Because PCA loadings can have arbitrary orientation, scores were rescaled so that higher values corresponded to greater vulnerability. We then performed a sensitivity analysis, comparing tract-level results across all three indices using Spearman's ρ and Kendall's τ rank correlations, overlap of the most vulnerable decile of tracts, and tercile reclassification matrices (Wolkin et al., 2022). This follows best practice in heat vulnerability research, where equal weighting and PCA are the most widely applied approaches (Li et al., 2022; Qian and Liu, 2025).

Table 2 shows that the index incorporated sensitivity and exposure indicators at the census tract level. Sensitivity refers to population characteristics that affect susceptibility to heat-related health impacts. Exposure refers to environmental conditions that indicate potential contact with extreme heat, with LST and population density as proxy measurements.

The selection of these indicators was guided by evidence from the literature demonstrating their associations with heat vulnerability. Age over 65, disability status, and living alone are established physiological and social risk factors (Méndez-Lázaro et al., 2018a; Osberghaus and Abeling, 2022). The “living alone” indicator reflects social isolation and reduced access to immediate assistance during heat events (Gossack-Keenan et al., 2024). Socioeconomic indicators (unemployment and low-income status) were included as they have shown to constrain to cooling resources and adaptive capacity (Li et al., 2023). Health insurance coverage was considered but excluded due to Puerto Rico's near-universal Medicaid (“plan vital”) eligibility, making it less discriminatory for vulnerability assessment (Puerto Rico, 2025). For exposure metrics, LST directly measures environmental heat, while population density captures increased urban heat retention in densely populated areas.

The index methodology synthesizes these environmental and social factors through PCA, with component weights validated through a comprehensive literature review. This approach maintains consistency with established vulnerability assessment protocols while adapting to Ponce's specific urban context. To develop the HVI, the variables selected were transformed into indices ranging from 0 to 1 using R (version 4.1.1) (Méndez-Lázaro et al., 2018a; Nayak et al., 2018; Reid et al., 2009). The directionality of each variable was considered so that higher values indicated greater vulnerability. This normalization process ensured consistency in measuring and comparing different variables.

The final index was constructed using a 50/50 weighting scheme to balance environmental and social determinants of heat vulnerability. 50 % of the index reflected urban heat exposure, and 50 % accounted for socioeconomic sensitivity factors. Specifically, LST and population density contributed 35 % and 15 % to the exposure dimension, respectively. Poverty, unemployment, age, disability, and living alone status collectively accounted for the remaining 50 % of the index. Each variable was standardized before aggregation to maintain the balance in weight.

Spatial analysis techniques were applied to map the distribution of the HVI at the census tract level ($n_{\text{census tracts}} = 45$). GIS software, ArcGIS 14.22.27821, was used to overlay the HVI scores onto a map of the city of Ponce. This highlighted areas with varying levels of

Table 2
Socio-demographic and thermal exposure indicators for heat vulnerability index development in the city of Ponce, Puerto Rico.

Category	Indicator	Unit	Spatial scale	Period	Source
Sensitivity					
Age	Percentage of population over 65	%	Census tracts	2018–2022	Census
Social Isolation	Percentage of population living alone (Single-person households)	%	Census tracts	2018–2022	Census
Socioeconomic	Population 16 years and over: in labor force, civilian labor force, unemployed	%	Census tracts	2018–2022	Census
Socioeconomic	Percentage of population characterized as low-income[a]	%	Census tracts	2018–2022	Census
Health	Percentage of population with a disability	%	Census tracts	2018–2022	Census
Exposure					
Population density	Density	Population per square mile	Census tracts	2018–2022	Census
Thermal stress exposure	Land surface temperature	°C	Census tracts	2013–2023	Landsat 8

[a] The 150 % of poverty estimate per census tract represents households whose income is 1.5 times (or 150 % of) the federal poverty level.

heat vulnerability. This spatial visualization helped identify hotspots where targeted interventions and policy measures can be implemented to mitigate the impacts of excessive heat.

3. Results

3.1. Spatial and statistical analysis of urban heat patterns

Fig. 2 presents the spatial distribution of vegetation cover (NDVI), land surface temperature (LST), elevation (DEM), and impervious surfaces across the city of Ponce. NDVI represents the annual mean from 2014 to 2023, while LST represents the mean for the warm season (June–September) from 2013 to 2023. Impervious surface data are from NOAA's 2022C-CAP product, and elevation is based on a static 10 m-resolution DEM from USGS. An inverse relationship is observed between vegetation density and urban development patterns (averaging 177-514 m above sea level, as shown in Fig. 2c). Higher-elevation areas have higher vegetation density, while the central urban core exhibits very low vegetation density.

Land surface temperature patterns (Fig. 2b) are inversely correlated with vegetation coverage and elevation. Warmer areas (42–45 °C) correspond primarily to densely developed lowland urban zones with mean elevations below 20 m (Fig. 2c). These areas are characterized by a high density of mixed-use buildings (including residential, commercial, and institutional structures), paved surfaces, and minimal vegetation (NDVI values <0.3). Cooler areas (31–34 °C) correspond to less developed, vegetated zones at higher elevations (exceeding 177 m; Fig. 2c). Here, NDVI values showed "Very High Vegetation Density". This thermal gradient illustrates the cooling effect of vegetation in urban environments and the temperature variations associated with topography census.

Fig. 3 illustrates the relationships between urban environmental characteristics through simple regression analyses. The analysis shows strong, significant correlations among vegetation coverage (NDVI), land surface temperature (LST), impervious surfaces, and

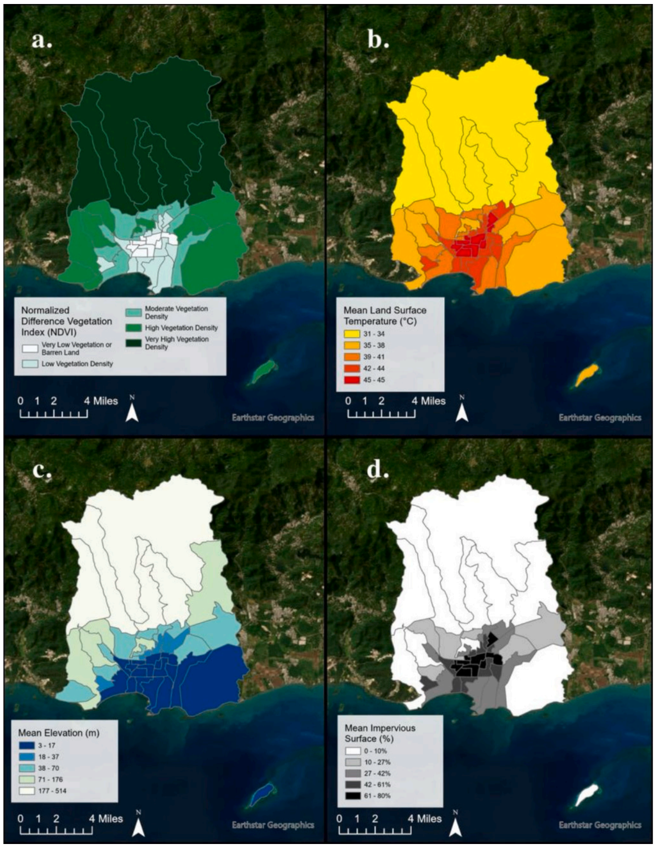

Fig. 2. Spatial distribution of vegetation, land surface temperature, elevation, and impervious surface by census tract in the city of Ponce, Puerto Rico. Panel (a) illustrates the Normalized Difference Vegetation Index (NDVI), derived from annual averages of Landsat 8 Operational Land Imager (OLI) data from 2014 to 2023, where darker green areas indicate census tracts with high vegetation density. Panel (b) shows the mean Land Surface Temperature (°C), calculated from Landsat 8 Thermal Infrared Sensor (TIRS) Band 10 data collected during June–September from 2013 to 2023 and aggregated to the census tract level. Panel (c) presents mean elevation (m), extracted from the USGS 10 m Digital Elevation Model (DEM), where darker blue tracts represent higher elevations. Panel (d) displays mean impervious surface (%) from NOAA's 2022 Coastal Change Analysis Program (C-CAP), where darker shades correspond to census tracts with higher percentages of built-up land cover (e.g., roads, buildings, and other impervious surfaces). (For interpretation of the references to colour in this figure legend, the reader is referred to the web version of this article.)

elevation across Ponce's census tracts. The NDVI values used in this analysis range from approximately −1 to 1, representing the census tract mean NDVI values, where higher values indicate greater vegetation density. A strong negative correlation exists between NDVI and LST, so census tracts with denser vegetation, primarily located in the highlands, exhibited lower surface temperatures. Instead, lowland urbanized areas with minimal vegetation showed significantly higher temperatures. Impervious surface coverage (Fig. 3b) had a strong positive correlation with LST, showing that highly urbanized lowland areas with extensive paved surfaces and buildings experience higher temperatures. In contrast, census tracts with lower impervious cover remained cooler in the highlands.

Elevation also played a role in moderating LST (Fig. 3c). Regions at greater altitudes exhibited significantly lower temperatures than densely developed lowland areas. These patterns highlight the combined influence of vegetation, urbanization, and topography on surface temperature variations in Ponce.

The multiple regression analysis examining the relationship between LST and urban environmental characteristics (Impervious Surface, NDVI, DEM, and slope) presented significant associations (all $p < 0.001$). The model demonstrated high explanatory power with an adjusted R-squared value of 0.84, indicating that these environmental and topographic variables collectively explain 84 % of the spatial variability in LST. Table 3 summarizes the regression coefficients and their interpretation. (See Tables 3 and 4.)

The north–south transect analysis confirmed a strong inverse relationship between elevation and surface temperature (Fig. 4). LST decreased consistently with altitude, indicating a clear topographic cooling effect.

3.2. Principal component analysis

Principal component analysis revealed three primary components explaining 85.4 % of the total variance in heat vulnerability across Ponce's census tracts (Table 3).

The first principal component (PC1) accounted for 45.4 % of the variance and primarily represents the intersection of high urban temperatures with social isolation and disability status. While Fig. 2 shows that the highest land surface temperatures are concentrated in the city's dense urban core, PC1 highlights specific census tracts where elevated temperatures statistically co-occur with higher proportions of residents living alone and with disabilities. This does not imply that all hot areas are socially isolated, but rather that PC1 isolates the areas where these dimensions most strongly overlap. PC2 explained 26.2 % of the variance and captured the co-occurrence of elderly populations with economic hardship. PC3, which explained 13.8 % of the variance, highlighted areas where high urban temperatures coincided with concentrations of poverty and disability.

3.3. Heat vulnerability index

The spatial analysis of social vulnerability factors across Ponce's census tracts illustrates how patterns of socioeconomic disparity (Fig. 5) match high vulnerability areas. In general, high vulnerability areas experienced land surface temperatures that averaged 44.28

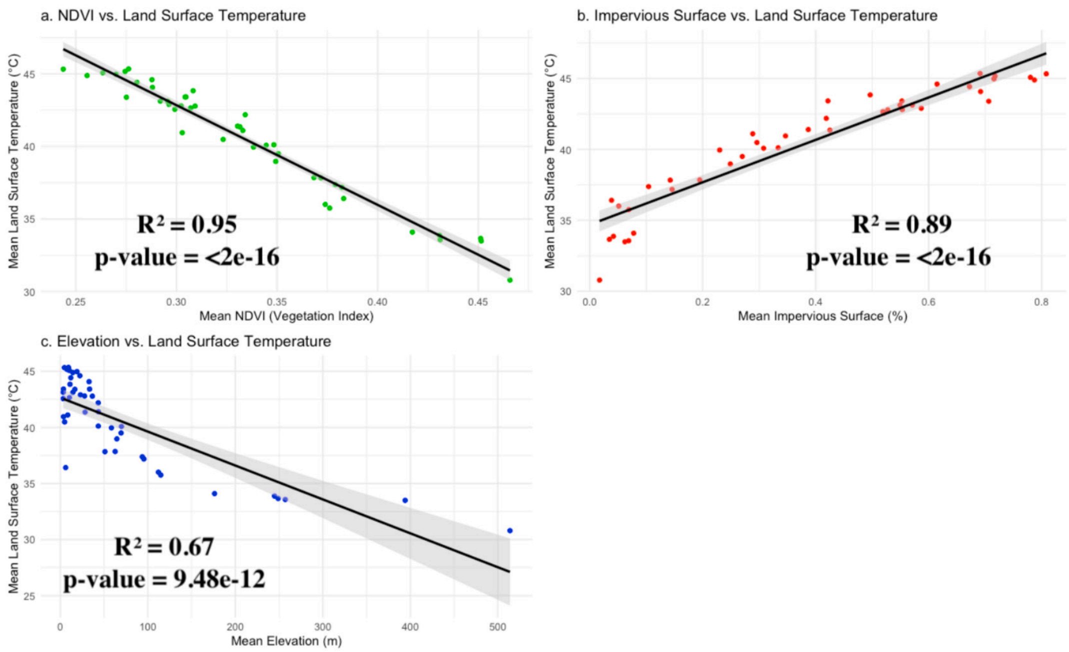

Fig. 3. Influence of elevation, vegetation (NDVI), and impervious surface on mean land surface temperature (LST) in the city of Ponce, Puerto Rico. All data were analyzed at the census tract level. LST values represent the average for the warm season (June–September) from 2013 to 2023, while NDVI represents the annual average from 2014 to 2023. Impervious surface data are from NOAA's 2022 Coastal Change Analysis Program (C-CAP), and elevation data are from the USGS 10 m Digital Elevation Model (DEM).

Table 3
Multiple regression coefficients showing the relationship between Land Surface Temperature (LST, °C) and environmental predictors, based on pixel-level data from the city of Ponce, Puerto Rico. LST represents the mean for the warm season (June–September) from 2013 to 2023, derived from Landsat 8 TIRS. NDVI is the annual average from 2014 to 2023, derived from Landsat 8 OLI. Impervious surface data are from NOAAs 2022C-CAP dataset, and elevation is from the USGS 10 m Digital Elevation Model (DEM). All variables were resampled to 30 m spatial resolution and analyzed at the pixel level.

Variable	Coefficient (β)	p-value	Interpretation
Impervious Surface (%)	0.7	<0.001	Higher imperviousness increases LST through urban heat retention.
NDVI	−2.57	<0.001	Higher vegetation density significantly reduces LST (cooling effect).
Elevation (m, DEM)	−1.92	<0.001	Higher elevation is associated with lower LST.
Slope (°)	−0.12	<0.001	Steeper terrain slightly lowers LST, reducing heat accumulation.

Table 3
Principal components of heat vulnerability in the city of Ponce, Puerto Rico.

Component	Explained Variance (%)	Dominant Variables	Interpretation
PC1	45.4	Percentage Living Alone (22.0 %), LST (20.4 %), Disabilities (14.6 %), Poverty (8.0 %)	Urban Heat & Social Isolation - Higher temperatures, low social support, and economic/health vulnerabilities.
PC2	26.2	Age 65+ (40.6 %), Unemployment (27.7 %), Poverty (18.2 %)	Elderly & Economic Disadvantage - Older populations with high unemployment and financial insecurity.
PC3	13.8	Poverty (29.9 %), LST (24.7 %), Disabilities (25.7 %)	Urban Density & Socioeconomic Constraints - High heat exposure combined with financial and health vulnerabilities.

Table 4
Socioeconomic and environmental characteristics across heat vulnerability zones in Ponce, Puerto Rico.

Indicator	Low Vulnerability	Moderate Vulnerability	High Vulnerability	Difference (%)[a]	p-value[b]
Population Density (people/sq. mi)	1116.33	4564.49	9210.73	725.1	1.25e-06
Poverty Rate (%)	66.95	64.66	76.42	14.1	0.58
Elderly Population (%)	21.66	27.04	26.05	20.3	0.026
Disability Rate (%)	21.66	26.16	26.51	22.4	0.029
Single-Person Households (%)	25.23	34.74	42.72	69.3	4.54e-05
Unemployment Rate (%)	11.22	10.55	22.55	101	0.056
Land Surface Temperature (°C)	35.89	41.48	44.19	23.1	3.15e-10

[a] Difference (%) shows percentage change between low and high vulnerability areas.
[b] Statistical comparisons between low and high vulnerability zones were conducted using independent t-tests for normally distributed variables and Wilcoxon rank-sum tests for non-normally distributed variables. P-values indicate the significance of differences between the two zones.

°C over those regions compared to 35.76 °C in low vulnerability zones ($p < 0.001$). Poverty levels, measured as the population living below 150 % of the federal poverty line, show significant concentration in the northern, southeastern, and central sections of the city, with some tracts experiencing poverty rates between 86 and 97 % (Fig. 5a). The unemployment distribution shows higher rates (32–54 %) in the lowlands and highlands (Fig. 5b), suggesting some spatial correlation with poverty patterns (Fig. 5a). Age vulnerability, represented by the population aged 65 and over, shows the highest concentrations (34–39 %) in the lowland census tracts (Fig. 5c). The disabled population exhibits a similar spatial pattern, with the highest percentages (33–39 %) also concentrated in the lowland region (Fig. 5d). Single-person households, an additional vulnerability indicator, showed notable clustering in the lowlands, with some tracts reaching 48–60 % (Fig. 5e).

The analysis of urban environment variables showed coincident spatial patterns in LST and population density across Ponce (Fig. 6). Mean land surface temperature showed a clear urban heat island effect, with the highest temperatures (42–45 °C) in the lowlands of Ponce (Fig. 6a). This pattern transitions to moderately high temperatures (39–41 °C) in the surrounding urban areas, with notably cooler temperatures (31–34 °C) in the less developed highlands. Population density distributions (Fig. 6b) closely mirror the urban development patterns, with the highest concentrations (10,254–15,486 people per mi^2) in the central urban area. Population density decreases outward from the center, with the lowest values (70–939 people per mi^2) in the northern areas.

The heat vulnerability index analysis for Ponce (Table 3, Fig. 7) shows that higher population density has higher vulnerability (8451.62 people/sq. mi compared to 1416.98 people/sq. mi in low vulnerability areas; $p < 0.001$). There is greater risk exposure in more densely populated neighborhoods.

The social profile of high vulnerability areas is characterized by concentrated disadvantage across multiple dimensions. These areas showed significantly higher percentages of elderly residents (26.40 % versus 21.71 %; $p = 0.027$) and of people with disabilities (26.19 % versus 22.25 %; $p = 0.029$). Single-person households were significantly more prevalent in high vulnerability areas (42.93 % compared to 26.30 % in low vulnerability areas; $p < 0.001$), representing one of the most pronounced social differences between areas. This social isolation factor is concerning as it can delay emergency responses during heat emergencies.

Although high vulnerability areas showed higher poverty rates (73.55 % versus 70.28 %) and substantially higher unemployment

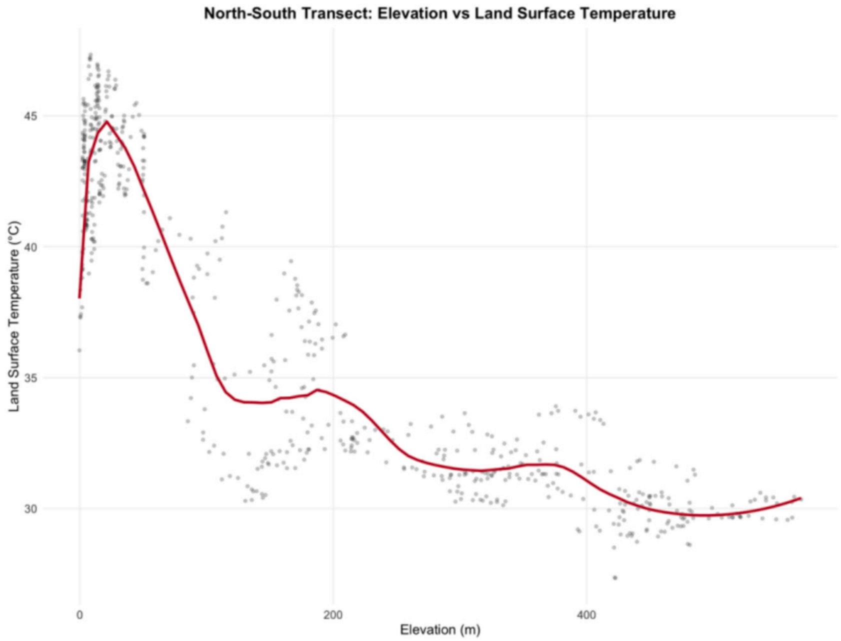

Fig. 4. Relationship between elevation and land surface temperature (LST) along a north–south transect across Ponce, Puerto Rico. The red line represents a moving-average curve that highlights the overall cooling trend with elevation. (For interpretation of the references to colour in this figure legend, the reader is referred to the web version of this article.)

rates (20.45 % versus 11.69 %; $p = 0.056$), the poverty difference with lower vulnerability areas did not reach statistical significance ($p = 0.579$). This suggested that, while economic factors contribute to vulnerability, they may interact with other social and environmental variables in complex ways.

These findings show how heat vulnerability in Ponce is defined by a systematic pattern in which social vulnerability factors coincide with environmental exposure. The most significant risks are concentrated in areas where higher proportions of elderly residents, persons with disabilities, and socially isolated individuals intersect with the urban heat island effect.

To test the robustness of these results, we constructed alternative indices. Sensitivity analyses showed that the equal-weights index was strongly correlated with our 50/50 HVI (Spearman $\rho = 0.92$; Kendall's $\tau = 0.76$), with 91 % overlap in the most vulnerable tracts. The PCA-weighted index had moderate correlation with the 50/50 HVI ($\rho = 0.76$; $\tau = 0.56$) but identified a different set of highest-risk tracts (0 % top-decile overlap). Despite these differences at the extremes, all three indices revealed consistent spatial patterns of moderate-to-high vulnerability across the city of Ponce.

4. Discussion

Our analysis demonstrated significant relationships between urban development patterns, social and economic factors, and thermal conditions in Ponce. The results also illustrated that built land cover patterns and urban form characteristics (impervious surface extent, vegetation cover, and topography) influence local climate. The strong correlations between land surface temperature, elevation, NDVI, impervious surfaces, and slope ($R^2 > 0.84$) highlighted the role of land cover composition and urban form in heat accumulation. The results reveal a clear urban heat island effect concentrated in the city's central core, where impervious surfaces are most prevalent and vulnerable populations, such as residents living alone, the elderly, and low-income communities, experience the highest exposure levels. These findings align with previous research in other urban areas and provide new insights into the unique challenges of small cities, where limited resources often constrain adaptation capabilities (Méndez-Lázaro et al., 2018a; Navarro-Estupiñan et al., 2020; Lazaro, 2015; Méndez-Lázaro et al., 2018b).

While the statistical disparities in population density, living alone status, and thermal exposure were expected, the non-significant difference in poverty rates between vulnerability zones presents an important distinction. Our data shows widespread poverty across Ponce, with poverty rates ranging from 36 % to nearly 97 % across census tracts. This pervasive economic hardship (*Pervasive Poverty in Puerto Rico: a Closer Look*, 2023) means that poverty affects most residents. This pattern differed from studies in continental U.S. cities, where economic status more consistently aligns with heat vulnerability (Benz and Burney, 2021).

Heat vulnerability and poverty intersect in Ponce, amplifying risk. Lower-income households often lack the resources for adequate cooling systems, live in homes with less insulation, and are located in areas with fewer green spaces. With poverty rates exceeding 53 %, these economic constraints create a cycle where extreme heat perpetuates existing inequities. Similarly, Ponce's elderly population (25.4 %, higher than the U.S. average) faces heightened risks due to diminished physiological capacity to regulate body temperature and a higher prevalence of chronic health conditions exacerbated by heat. Individuals with disabilities may face mobility limitations

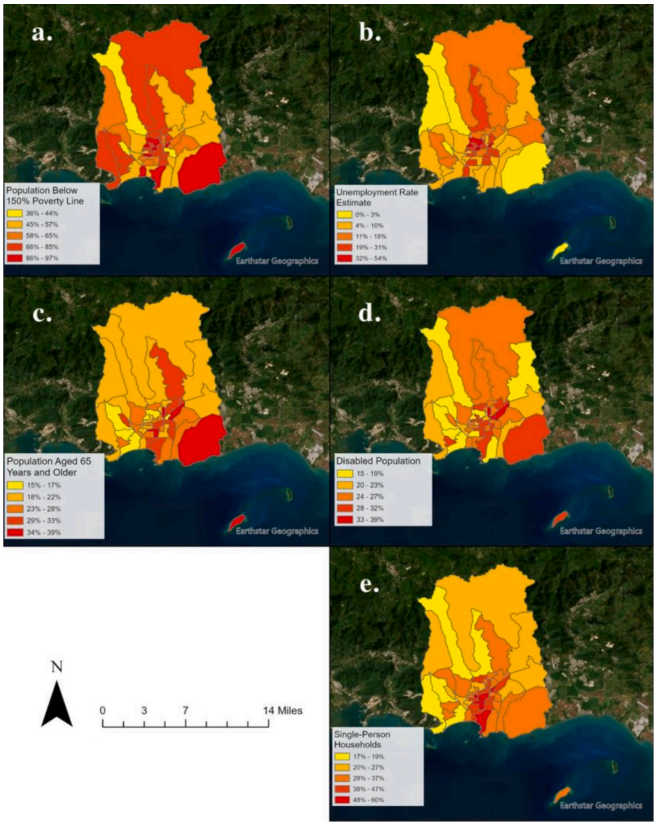

Fig. 5. Spatial distribution of socioeconomic vulnerability indicators. Panel (a) represents the percentage of the population living below 150 % of the poverty line. Panel (b) displays the unemployment rate. Panel (c) maps the percentage of the population aged 65 and over. Panel (d) shows the percentage of the population with disabilities. Lastly, panel (e) presents the percentage of single-person households. Each map employs a graduated colour scheme: yellow represents lower percentages, and red indicates higher concentrations. (For interpretation of the references to colour in this figure legend, the reader is referred to the web version of this article.)

affecting their ability to relocate to cooler environments, while those living alone lack immediate social support during emergencies.

Unlike San Juan, which benefits from greater resources and infrastructure investments, Ponce's vulnerability is compounded by limited adaptation capacity and higher energy instability (Redacción, 2024; *Fin de Semana Sin Luz para Sectores de San Juan y Ponce – Metro Puerto Rico*, 2025; *Sin Luz Gran Parte de Ponce - Primera Hora*, 2025; *Camión Deja Sin Luz a Comunidad de Ponce – Telemundo Puerto Rico*, 2025; *Alcaldesa de ponce advierte que LUMA está "matando a nuestra gente"*, 2025). Similar heat vulnerability patterns have been observed in other Latin American cities, such as Hermosillo, Mexico (Navarro-Estupiñan et al., 2020), though with important regional differences in how social and environmental factors interact to create vulnerability. Understanding how heat risk is distributed across different population groups enables adaptation planning that prioritizes the most vulnerable rather than applying uniform strategies across the city.

This study has some limitations. While valuable for assessing urban heat patterns, land surface temperature estimates do not fully capture indoor thermal conditions or neighborhood-scale microclimate variations. Our analysis was also constrained by the spatial resolution of thermal satellite data, the limited availability of cloud-free imagery during peak heat periods, and the absence of ground-based temperature monitoring that would provide continuous data, including nighttime temperatures, when heat stress can persist. A limitation is the lack of data on household access to air conditioning (A/C). While air conditioning is a crucial adaptation measure for extreme heat, the U.S. Census Bureau does not collect this information for Puerto Rico. Such a metric is included for the U.S. territory of Guam (*HBG51: Air Conditioning - Census Bureau Table*, 2025). Similarly, detailed housing structure characteristics, such as roof type, wall materials, ventilation, and the presence or absence of ceilings, are not available at the census tract level in Puerto Rico. These variables strongly influence indoor heat exposure and would significantly enhance future heat vulnerability assessments.

Like other municipalities in Puerto Rico, Ponce experiences frequent power outages. This exacerbates heat vulnerability by limiting access to cooling options, refrigeration, and other important services. These power disruptions, often lasting for extended periods, are particularly concerning for vulnerable populations, including the elderly and those with chronic illnesses who rely on electrically powered medical devices. The interplay between extreme heat, unreliable electricity, and social vulnerability highlights the need to strengthen infrastructure resilience and expand cooling access.

Future research could explore alternative datasets, surveys, or qualitative methods to assess A/C availability and its role in

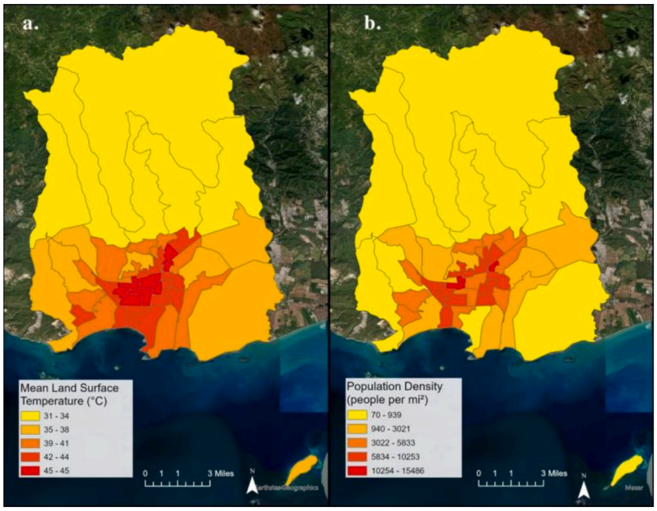

Fig. 6. Spatial distribution of mean land surface temperature and population density in the city of Ponce, Puerto Rico. Panel (a) illustrates the Mean Land Surface Temperature (°C), derived from Landsat 8 TIRS data, highlighting temperature variations across the urban landscape. Warmer areas, shown in red, correspond to regions with higher temperatures, whereas yellow areas indicate cooler zones. Panel (b) illustrates Population Density (people per mi^2), based on U.S. Census data, identifying areas of high population concentration. Higher density areas, shown in red, overlap with zones experiencing elevated land surface temperatures. (For interpretation of the references to colour in this figure legend, the reader is referred to the web version of this article.)

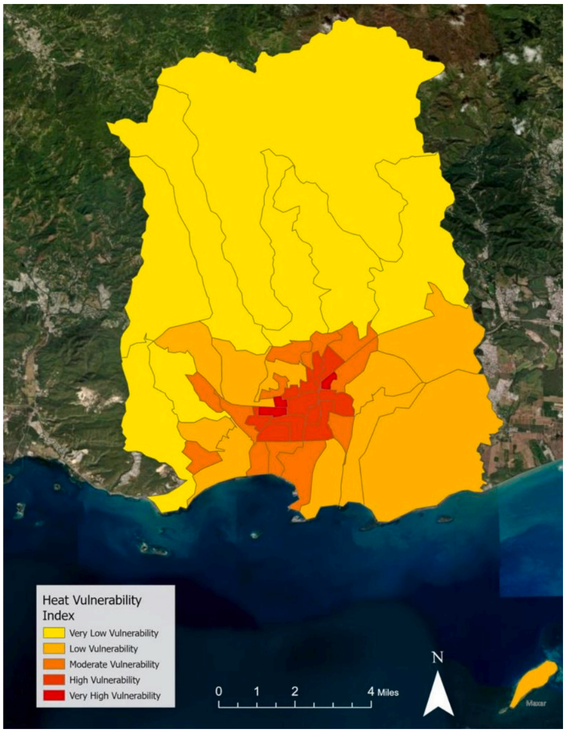

Fig. 7. Heat vulnerability index (HVI) for the city of Ponce, Puerto Rico. This map presents the spatial distribution of the Heat Vulnerability Index (HVI) across census tracts in the city of Ponce, Puerto Rico. Areas classified as Very High Vulnerability (red) represent communities facing the greatest risk from extreme heat, while Very Low Vulnerability (yellow) indicates areas with lower susceptibility. (For interpretation of the references to colour in this figure legend, the reader is referred to the web version of this article.)

mitigating heat stress. This may include ground-based temperature monitoring, finer-scale terrain analyses (slope, aspect) to capture microclimatic variability, community engagement, and health outcome data to enhance understanding of heat-related risks. Examining longitudinal trends in temperature and adaptation effectiveness would provide insights into how to adapt urban management.

5. Conclusion

This study represents an initial step toward understanding heat vulnerability in Ponce by identifying where social and environmental risk factors intersect. By integrating spatial analysis with social vulnerability indicators, the findings provide actionable insights to inform data-driven decision-making and prioritize future interventions. The heat vulnerability maps developed through this research offer practical tools for local policymakers and emergency management agencies to target resources where they are most needed. Municipal governments may use these findings to develop heat action plans that include early warning systems tailored to Ponce's highest-risk neighborhoods, investment in cooling centers in vulnerable communities, and strategic urban greening initiatives in areas with the highest land surface temperatures. The quantification of cooling effects from vegetation suggests specific targets for urban forestry programs and green infrastructure development in high-vulnerability census tracts. Establishing formal collaborative frameworks between academic researchers, the Municipality of Ponce's Planning and Public Health Departments, Puerto Rico's Department of Health, and community-based organizations serving vulnerable populations represents a promising direction for future work. Such partnerships could facilitate the integration of heat vulnerability assessments into municipal climate adaptation plans, emergency response protocols, and infrastructure investment decisions. Expanding this methodology to other municipalities across Puerto Rico would enable regional coordination of heat mitigation strategies and more efficient allocation of limited adaptation resources. While the study does not directly mitigate vulnerabilities, it lays the groundwork for targeted policy responses, investment in cooling infrastructure, and further research in other municipalities facing similar climate challenges.

Based on the spatial patterns identified in this study, several strategies may help reduce heat vulnerability in Ponce. Targeted urban greening in high-temperature census tracts, reflective roofing and pavement materials, and expanded cooling centers could help mitigate extreme heat exposure. Decentralized energy solutions, such as microgrids and solar-powered cooling hubs, may strengthen resilience during frequent power outages. Establishing dedicated municipal heat governance, such as a Heat Resilience Officer, could improve coordination of early warning systems, emergency response, and support for socially isolated or medically vulnerable residents. These recommendations follow directly from the vulnerability patterns observed and may guide the municipality's heat adaptation planning.

CRediT authorship contribution statement

Laura T. Cabrera-Rivera: Writing – review & editing, Writing – original draft, Visualization, Methodology, Investigation, Formal analysis, Data curation, Conceptualization. **Frank E. Muller-Karger:** Writing – review & editing, Conceptualization. **Digna Rueda-Roa:** data analysis, writing, and manuscript review. **Heriberto Marin:** Writing – review & editing, Conceptualization. **Tischa A. Muñoz-Erickson:** Writing – review & editing, Conceptualization. **Pablo A. Méndez-Lázaro:** Writing – review & editing, Validation, Supervision, Resources, Project administration, Funding acquisition, Conceptualization.

Declaration of competing interest

The authors declare that they have no known competing financial interests or personal relationships that could have appeared to influence the work reported in this paper.

The author is an Editorial Board Member/Editor-in-Chief/Associate Editor/Guest Editor for *[Journal name]* and was not involved in the editorial review or the decision to publish this article.

The authors declare the following financial interests/personal relationships which may be considered as potential competing interests:

Acknowledgments

This research was supported by the National Oceanic and Atmospheric Administration (NOAA) through the Climate Adaptation Partnerships (CAP) program under Grant Number NA22OAR4310545. Additional support was provided by the USDA Forest Service, International Institute of Tropical Forestry. The findings and conclusions in this publication are those of the authors and should not be construed to represent official USDA or U.S. determination or policy.

Data availability

The datasets used and/or analyzed during the current study are publicly available.

References

Aboulnaga, M., Trombadore, A., Mostafa, M., Abouaiana, A., 2024. Livability: The Direction to Mitigating Urban Heat Islands' Effect, Achieving Healthy, Sustainable, and Resilient Cities, and the Coverage. Springer International Publishing, Livable Cities, Cham, pp. 1–282. https://doi.org/10.1007/978-3-031-51220-9_1.

Alcaldesa de ponce advierte que LUMA está “matando a nuestra gente”. In: Agencias, 2025. elvocero.com. https://www.elvocero.com/gobierno/agencias/alcaldesa-de-ponce-advierte-que-luma-est-matando-a-nuestra-gente/article_0e85c0c8-279d-11ef-9d9e-af8812bb88ba.html (accessed March 26, 2025).

Benz, S.A., Burney, J.A., 2021. Widespread race and class disparities in surface urban heat extremes across the United States. Earth’s Future 9, e2021EF002016. https://doi.org/10.1029/2021EF002016.

Bu, S., Smith, K.L., Masoud, F., Sheinbaum, A., 2024. Spatial distribution of heat vulnerability in Toronto, Canada. Urban Clim. 54, 101838. https://doi.org/10.1016/j.uclim.2024.101838.

Bureau UC, 2025. Puerto Rico Municipios Population Totals: 2020-2023. CensusGov. https://www.census.gov/data/tables/time-series/demo/popest/2020s-total-puerto-rico-municipios.html (accessed February 10, 2025).

Camión Deja Sin Luz a Comunidad de Ponce – Telemundo Puerto Rico. https://www.telemundopr.com/noticias/puerto-rico/camion-deja-sin-luz-a-comunidad-de-ponce/2403948/, 2025 (accessed March 26, 2025).

Conlon, K.C., Mallen, E., Gronlund, C.J., Berrocal, V.J., Larsen, L., O’Neill, M.S., 2020. Mapping human vulnerability to extreme heat: a critical assessment of heat vulnerability indices created using principal components analysis. Environ. Health Perspect. 128, 097001. https://doi.org/10.1289/EHP4030.

Cook, M., Schott, J., Mandel, J., Raqueno, N., 2014. Development of an operational calibration methodology for the Landsat thermal data archive and initial testing of the atmospheric compensation component of a land surface temperature (LST) product from the archive. Remote Sens. 6, 11244–11266. https://doi.org/10.3390/rs61111244.

Copernicus, 2025. Copernicus: 2024 is the First Year to Exceed 1.5°C Above Pre-industrial Level. Copernicus. https://climate.copernicus.eu/copernicus-2024-first-year-exceed-15degc-above-pre-industrial-level# (accessed January 13, 2025).

Devanathan, P., Devanathan, K., 2011. Heat island effects. In: Green Building with Concrete: Sustainable Design Construction, pp. 175–226.

Fin de Semana Sin Luz para Sectores de San Juan y Ponce – Metro Puerto Rico. https://www.metro.pr/noticias/2024/07/27/fin-de-semana-sin-luz-para-sectores-de-san-juan-y-ponce/, 2025 (accessed March 26, 2025).

Giraldo-Santiago, N., Alvarez-Hernandez, L.R., Machado-Escudero, Y., Zhen-Duan, J., 2024. Factors associated with thoughts of migration among Latinx mental health professionals from Puerto Rico to mainland United States. Clin. Soc. Work. J. https://doi.org/10.1007/s10615-024-00920-7.

Gossack-Keenan, K., Yeom, D.S., Kanu, J., Hau, J.P., Rosychuk, R.J., Clark, D., et al., 2024. Heatstroke presentations to urban hospitals during BC’S extreme heat event: lessons for the future. Can. J. Emerg. Med. 26, 111–118. https://doi.org/10.1007/s43678-023-00622-y.

HBG51: Air Conditioning - Census Bureau Table. https://data.census.gov/table/DECENNIALGU2010.HBG51?q=AIR%20ON%20DEMAND, 2025 (accessed February 12, 2025).

He, B.-J., Zhao, D., Dong, X., Xiong, K., Feng, C., Qi, Q., et al., 2022. Perception, physiological and psychological impacts, adaptive awareness and knowledge, and climate justice under urban heat: a study in extremely hot-humid Chongqing, China. Sustain. Cities Soc. 79, 103685. https://doi.org/10.1016/j.scs.2022.103685.

Hulley, G., Shivers, S., Wetherley, E., Cudd, R., 2019. New ECOSTRESS and MODIS land surface temperature data reveal fine-scale heat vulnerability in cities: a case study for Los Angeles County, California. Remote Sens. 11, 2136. https://doi.org/10.3390/rs11182136.

Interactive Atlas of Heart Disease and Stroke. https://nccd.cdc.gov/DHDSPAtlas/Default.aspx?state=PR, 2025 (accessed April 13, 2024).

Ipcc, 2022. Global Warming of 1.5°C: IPCC Special Report on Impacts of Global Warming of 1.5°C above Pre-Industrial Levels in Context of Strengthening Response to Climate Change, Sustainable Development, and Efforts to Eradicate Poverty, 1st ed. Cambridge University Press. https://doi.org/10.1017/9781009157940.

Ji, H., Shin, S.H., Coronado, A., Lee, H.Y., 2025. Extreme heat, functional disability, and social isolation: risk disparity among older adults. J. Appl. Gerontol. 44, 561–570. https://doi.org/10.1177/07334648241282904.

Kim, S.W., Brown, R.D., 2021. Urban heat island (UHI) variations within a city boundary: a systematic literature review. Renew. Sust. Energ. Rev. 148, 111256. https://doi.org/10.1016/j.rser.2021.111256.

Lazaro, P.M., 2015. Extreme heat events in San Juan Puerto Rico: trends and variability of unusual hot weather and its possible effects on ecology and society. J. Climatol. Weather Forecast. 03. https://doi.org/10.4172/2332-2594.1000135.

Li, F., Yigitcanlar, T., Nepal, M., Thanh, K., Dur, F., 2022. Understanding urban heat vulnerability assessment methods: a PRISMA review. Energies 15, 6998. https://doi.org/10.3390/en15196998.

Li, A., Toll, M., Bentley, R., 2023. Mapping social vulnerability indicators to understand the health impacts of climate change: a scoping review. Lancet Planet. Heath 7, e925–e937. https://doi.org/10.1016/S2542-5196(23)00216-4.

Meenar, M., Rahman, M.S., Russack, J., Bauer, S., Kapri, K., 2023. “The urban poor and vulnerable are hit hardest by the heat”: a heat equity lens to understand community perceptions of climate change, urban heat islands, and green infrastructure. Land 12, 2174. https://doi.org/10.3390/land12122174.

Méndez-Lázaro, P., 2023. Chapter 23 : US Caribbean. In: Fifth National Climate Assessment. U.S. Global Change Research Program. https://doi.org/10.7930/NCA5.2023.CH23.

Méndez-Lázaro, P., Muller-Karger, F.E., Otis, D., McCarthy, M.J., Rodríguez, E., 2018a. A heat vulnerability index to improve urban public health management in San Juan, Puerto Rico. Int. J. Biometeorol. 62, 709–722. https://doi.org/10.1007/s00484-017-1319-z.

Méndez-Lázaro, P.A., Pérez-Cardona, C.M., Rodríguez, E., Martínez, O., Taboas, M., Bocanegra, A., et al., 2018b. Climate change, heat, and mortality in the tropical urban area of San Juan, Puerto Rico. Int. J. Biometeorol. 62, 699–707. https://doi.org/10.1007/s00484-016-1291-z.

Mohajerani, A., Bakaric, J., Jeffrey-Bailey, T., 2017. The urban heat island effect, its causes, and mitigation, with reference to the thermal properties of asphalt concrete. J. Environ. Manag. 197, 522–538. https://doi.org/10.1016/j.jenvman.2017.03.095.

NASA, 2025. Temperatures Rising: NASA Confirms 2024 Warmest Year on Record - NASA. https://www.nasa.gov/news-release/temperatures-rising-nasa-confirms-2024-warmest-year-on-record/ (accessed January 13, 2025).

Navarro-Estupiñan, J., Robles-Morua, A., Díaz-Caravantes, R., Vivoni, E.R., 2020. Heat risk mapping through spatial analysis of remotely-sensed data and socioeconomic vulnerability in Hermosillo, México. Urban Clim. 31, 100576. https://doi.org/10.1016/j.uclim.2019.100576.

Nayak, S.G., Shrestha, S., Kinney, P.L., Ross, Z., Sheridan, S.C., Pantea, C.I., et al., 2018. Development of a heat vulnerability index for New York state. Public Health 161, 127–137. https://doi.org/10.1016/j.puhe.2017.09.006.

Niggli, L., Huggel, C., Muccione, V., Neukom, R., Salzmann, N., 2022. Towards improved understanding of cascading and interconnected risks from concurrent weather extremes: analysis of historical heat and drought extreme events. PLOS Clim. 1, e0000057. https://doi.org/10.1371/journal.pclm.0000057.

Niu, Y., Li, Z., Gao, Y., Liu, X., Xu, L., Vardoulakis, S., et al., 2021. A systematic review of the development and validation of the heat vulnerability index: major factors, methods, and spatial units. Curr. Clim. Chang. Rep. 7, 87–97. https://doi.org/10.1007/s40641-021-00173-3.

NOAA, 2025. 2024 was the world’s warmest year on record. In: National Oceanic and Atmospheric Administration. https://www.noaa.gov/news/2024-was-worlds-warmest-year-on-record (accessed January 13, 2025).

Osberghaus, D., Abeling, T., 2022. Heat vulnerability and adaptation of low-income households in Germany. Glob. Environ. Chang. 72, 102446. https://doi.org/10.1016/j.gloenvcha.2021.102446.

Pervasive Poverty in Puerto Rico: a Closer Look, 2023. CentroPR. https://centropr.hunter.cuny.edu/reports/pervasive-poverty-in-puerto-rico/ (accessed March 18, 2025).

Ponce Latitude Longitude. https://latitudelongitude.org/pr/ponce/, 2025 (accessed March 4, 2024).

Puerto Rico, 2025. Medicaid.gov. https://www.medicaid.gov/state-overviews/puerto-rico.html (accessed April 15, 2025).

Puerto Rico Climate Change Council (PRCCC), 2022. Puerto Rico’s state of the climate 2014-2021: Assesing Puerto Rico’s social-ecological vulnerabilities in a changing climate. In: San Juan, PR: Puerto Rico Coastal Zone Management Program, Department of Natutral and Environmental Resources, NOAA Office of Ocean and Coastal Resource Management.

Puleikis, K., Wang, J., 2023. Puerto Rico historical climate analysis: a closer look at complex tropical terrain. In: Argonne National Laboratory (ANL), Argonne, IL (United States). https://doi.org/10.2172/1974354.

Qian, Y., Liu, T., 2025. Heat vulnerability assessment: a systematic review of critical metrics. Hyg. Environ. Health Adv. 15, 100138. https://doi.org/10.1016/j.heha.2025.100138.

Redacción, L., 2024. Ponce es la región con mayor cantidad de clientes sin luz. Period. La Perla. https://www.periodicolaperla.com/actualidad/ponce-es-la-region-con-mayor-cantidad-de-clientes-sin-luz/ (accessed March 26, 2025).

Reid, C.E., O'Neill, M.S., Gronlund, C.J., Brines, S.J., Brown, D.G., Diez-Roux, A.V., et al., 2009. Mapping community determinants of heat vulnerability. Environ. Health Perspect. 117, 1730–1736. https://doi.org/10.1289/ehp.0900683.

Reyes Cruz, C.A., 2023. Causes of Displacement: A Look into the State of Puerto Rico's Housing Crisis Before, during, and after Hurricane Maria.

Rizwan, A.M., Dennis, L.Y.C., Liu, C., 2008. A review on the generation, determination and mitigation of urban heat island. J. Environ. Sci. 20, 120–128. https://doi.org/10.1016/S1001-0742(08)60019-4.

Sánchez-Celada, M., 2018. Áreas Bajo Estrés en Sitios Seleccionados para Puerto Rico, Centros Históricos Urbanos de San Juan y Puerto Rico. Editorial Académica Española.

Sin Luz Gran Parte de Ponce - Primera Hora. https://www.primerahora.com/noticias/puerto-rico/notas/sin-luz-gran-parte-de-ponce/, 2025 (accessed March 26, 2025).

U.S. Census Bureau QuickFacts: Ponce Municipio, Puerto Rico. https://www.census.gov/quickfacts/poncemunicipiopuertorico, 2025 (accessed February 22, 2023).

US Department of Commerce N. PR and USVI Normals, 2025. https://www.weather.gov/sju/climo_pr_usvi_normals (accessed March 20, 2024).

WMO, 2025. WMO Confirms 2024 as Warmest Year on Record at About 1.55°C Above Pre-industrial Level 2025. https://wmo.int/news/media-centre/wmo-confirms-2024-warmest-year-record-about-155degc-above-pre-industrial-level# (accessed January 13, 2025).

Wolkin, A., Collier, S., House, J.S., Reif, D., Motsinger-Reif, A., Duca, L., et al., 2022. Comparison of national vulnerability indices used by the centers for disease control and prevention for the COVID-19 response. Public Health Rep. 137, 803–812. https://doi.org/10.1177/00333549221090262.

Zhou, Y., Xia, Y., Chen, B., Fujino, Y., 2020. Analytical solution to temperature-induced deformation of suspension bridges. Mech. Syst. Signal Process. 139, 106568. https://doi.org/10.1016/j.ymssp.2019.106568.